Supporting Information

Mimicking anthocephalus cadamba shaped FeNi encapsulated carbon nanostructures for metal-air batteries as resilient bifunctional oxygen electrocatalyst

Ravi Nandan,[a] Ajay Gautam[a] and Karuna Kar Nanda[a,]*

[a]Materials Research Centre, Indian institute of Science, Bangalore-560012, India.

Fax: +91-80-2360 7316; Ph: +91-80-2293 2996

*E-mail: nanda@iisc.ac.in (Prof. K. K. Nanda)

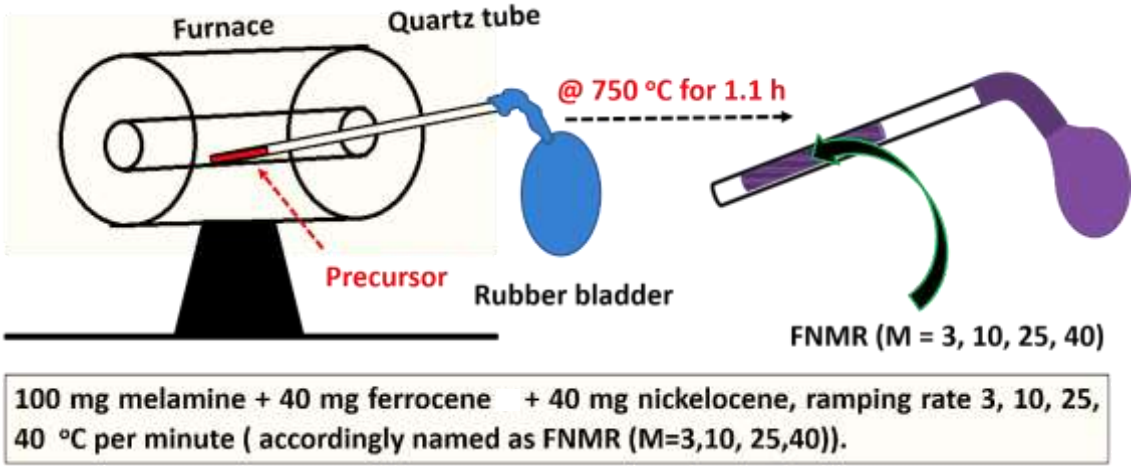

Figure S1. Schematic representation of FNMR (M= 3, 10, 25, 40) synthesis**.** The close end of the precursor loaded quartz tube was kept at the middle position of the furnace followed by pyrolysis at 750 ^{o}C for 1.1 h.

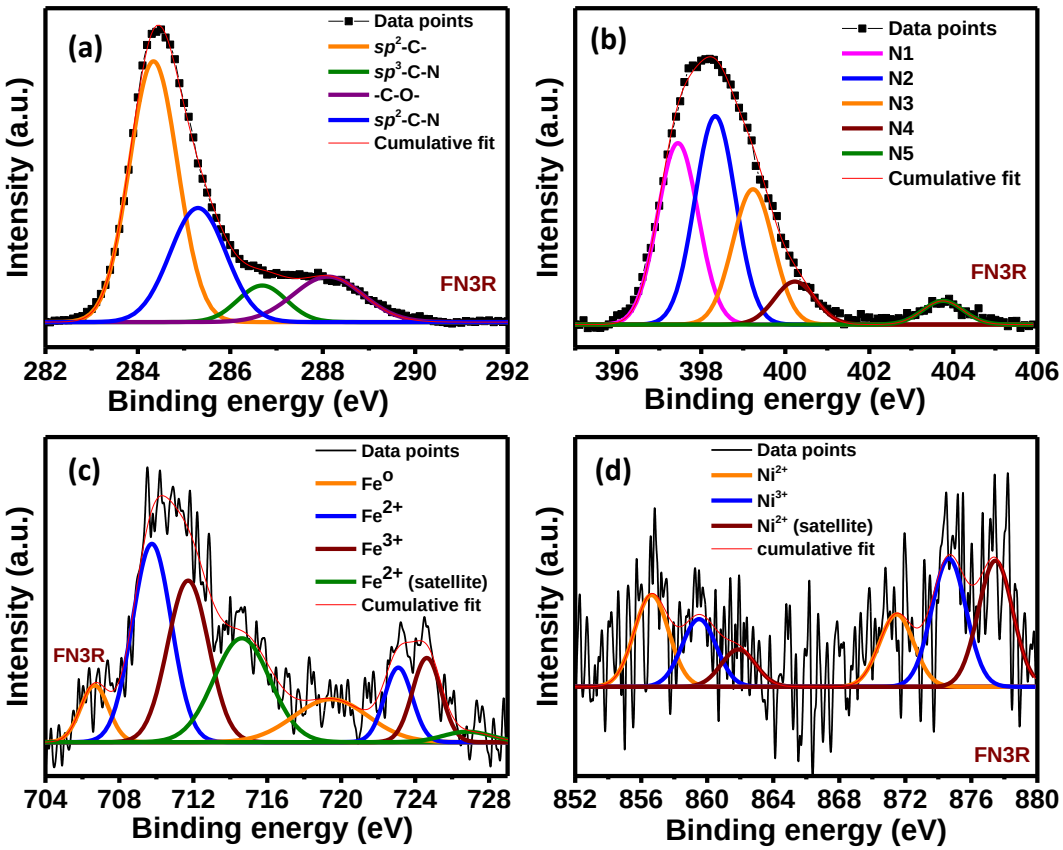

Figure S2. Deconvoluted HRXPS core spectra of FN3R for (a) C1s, (b) N1s, (c) Fe (2p) and (d) Ni2p, respectively.

Figure S2a shows the deconvoluted C1s core spectrum of FN3R comprises of peaks centred around 284.4, 285.3, 286.6 and 288.1 eV which can be assigned to to sp^2-*C*, sp^2 *C-N*, sp^3 *C-N* and carbon-oxygen functionalities, respectively.[1-3] Depending upon the nitrogen chemical environment and interactions with other elements, the deconvolution of N1s spectrum suggests the presence of pyridinic (N1~397.4), pyrrolic (N3~399.2 eV), quaternary (N4~400.2 eV) and some oxygenated nitrogen (N5~403.7 eV) functionalities, in addition to the metal-nitrogen coordinated functionalities M-NxC (M= Fe, Ni) with characteristic binding energy of 398.6±0.3 eV (N2).[1-4] The deconvolution of Fe2p core spectrum (Figure. S2c) suggests the presence of the peaks centred around 706.6, 709.7, 711.7 eV can be attributed to the Fe^o, Fe^{2+}, Fe^{3+} $2p_{3/2}$ state whereas peaks centred around 719.4, 723, 724.6 eV can be attributed to the Fe^o, Fe^{2+}, Fe^{3+} $2p_{1/2}$ states.[1-8] Besides, Fe^{2+} satellite peaks at 714.6 eV ($2p_{3/2}$) and 726.8 ev ($2p_{1/2}$) has been

observed.[6] Similarly, the peaks centred around 856.6, 859.5 eV can be attributed to the Ni^{2+}, Ni^{3+} $2p_{3/2}$ state whereas peaks centred around 871.4, 874.6 eV can be attributed to the Ni^{2+}, Ni^{3+} $2p_{1/2}$ states.[6-13] In addition, Ni^{2+} satellite peaks at 861.8 eV ($2p_{3/2}$) and 877.4 ev ($2p_{1/2}$) has been also observed.[6]

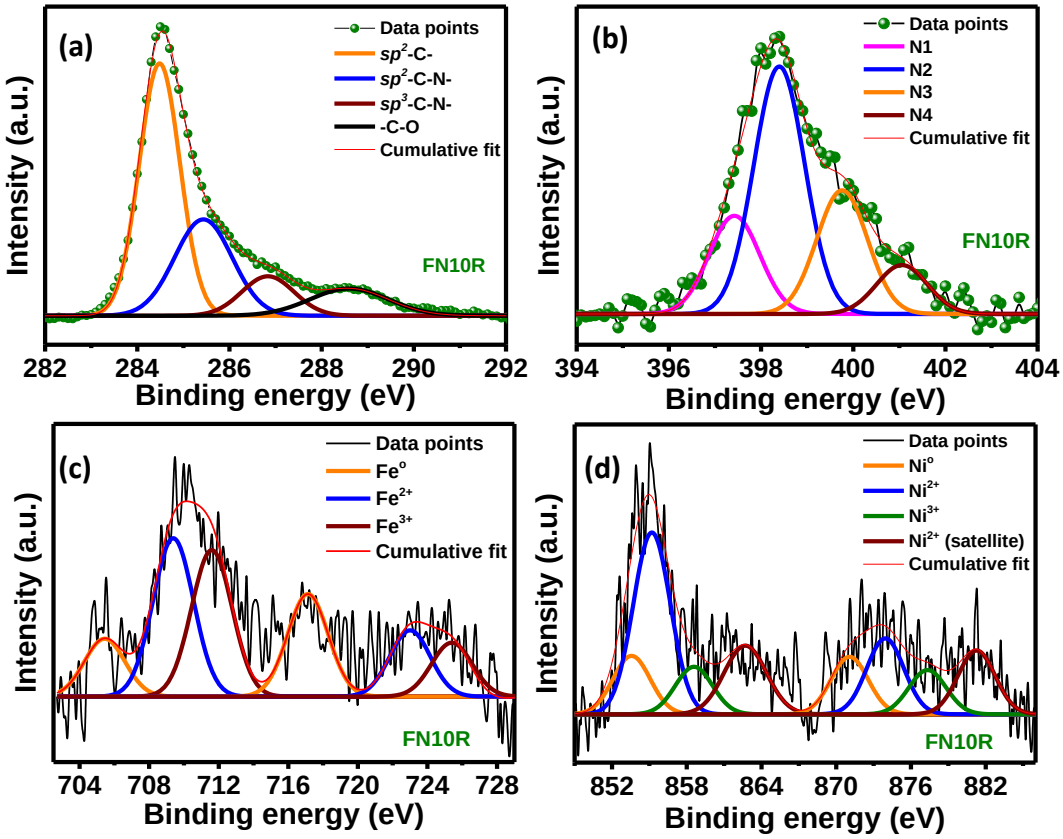

Figure S3. Deconvoluted HRXPS core spectra of FN10R for (a) C1s, (b) N1s, (c) Fe (2p) and (d) Ni2p, respectively.

Figure S3a shows the deconvoluted C1s core spectrum of FN10R comprises of peaks centred around 284.48, 285.4, 286.8 and 288.6 eV which can be assigned to to sp^2-*C*, sp^2 *C-N*, sp^3 *C-N* and carbon-oxygen functionalities, respectively.[1-3] Depending upon the nitrogen chemical environment and interactions with other elements, the deconvolution of N1s spectrum (Figure. S3b) suggests the presence of pyridinic (N1~397.4), pyrrolic (N3~399.7 eV), quaternary (N4~401 eV) functionalities, in addition to the metal-nitrogen coordinated functionalities M-

NxC (M= Fe, Ni) with characteristic binding energy of 398.6±0.3 eV (N2).[1-4] The deconvolution of Fe2p core spectrum (Figure S3c) suggests the presence of the peaks centred around 705.4, 709.3, 711.6 eV can be attributed to the Fe^{o}, Fe^{2+}, Fe^{3+} $2p_{3/2}$ state whereas peaks centred around 717.1, 723.2, 725.4 eV can be attributed to the Fe^{o}, Fe^{2+}, Fe^{3+} $2p_{1/2}$ states.[1-8] Similarly, the peaks centred around 853.5, 855.2, 858.5 eV can be attributed to the Ni^{o}, Ni^{2+}, Ni^{3+} $2p_{3/2}$ state whereas peaks centred around 871.2, 873.9, 877.3 eV can be attributed to the Ni^{o}, Ni^{2+}, Ni^{3+} $2p_{1/2}$ states.[6-13] In addition, Ni^{2+} satellite peaks at 862.7 eV ($2p_{3/2}$) and 88.2 ev ($2p_{1/2}$) has been also observed.[6]

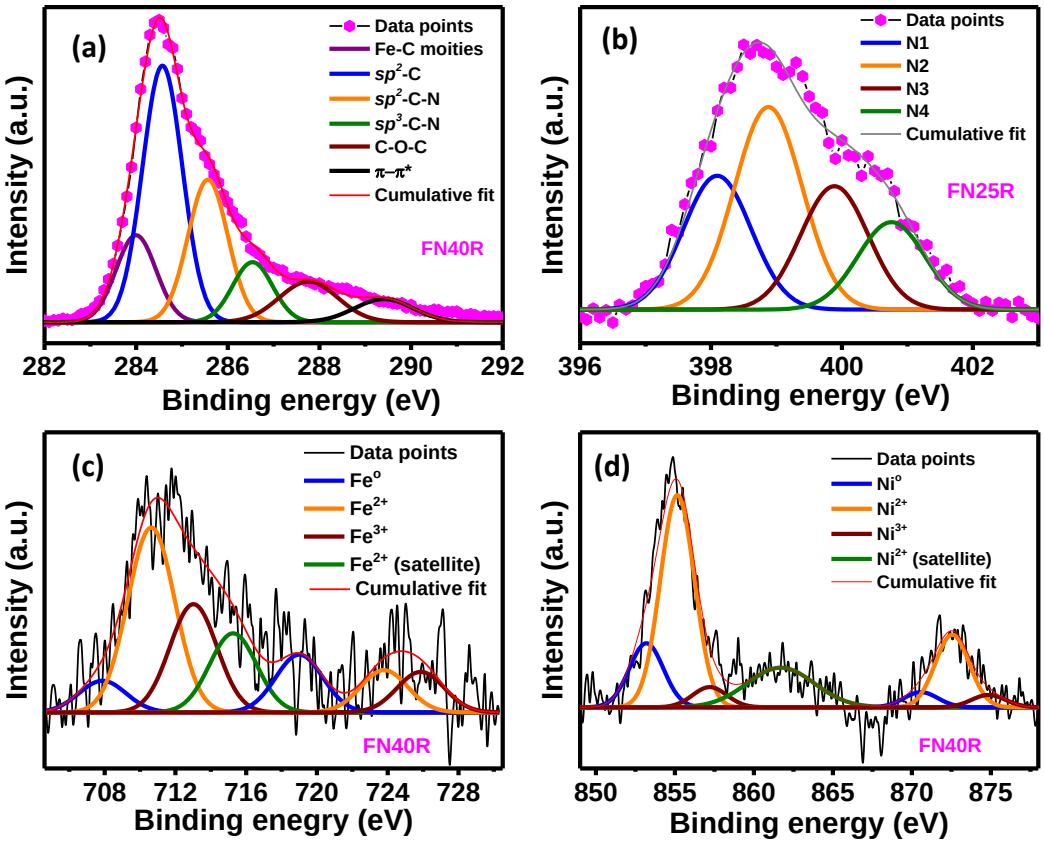

Figure S4. Deconvoluted HRXPS core spectra of FN40R for (a) C1s, (b) N1s, (c) Fe (2p) and (d) Ni2p, respectively.

Figure S4a shows the deconvoluted C1s core spectrum of FN40R comprises of peaks centred around 283.9, 284.5, 285.5, 286.8, 286.5, 287.7 and 289.4 eV which can be assigned to to *Fe-*

C, sp^2-*C*, sp^2 *C-N*, sp^3 *C-N*, carbon-oxygen (C-O-C) functionalities and π–π∗ satellite peak, respectively.[1-3] Depending upon the nitrogen chemical environment and interactions with other elements, the deconvolution of N1s spectrum (Figure. S4b) suggests the presence of pyridinic (N1~398), pyrrolic (N3~399.8 eV) and quaternary (N4~400.7 eV) functionalities, in addition to the metal-nitrogen coordinated functionalities M-NxC (M= Fe, Ni) with characteristic binding energy of 398.6±0.3 eV (N2).[1-4] The deconvolution of Fe2p core spectrum (Figure. S4c) suggests the presence of the peaks centred around 707.8, 710.6, 713.1 eV can be attributed to the Fe^o, Fe^{2+}, Fe^{3+} $2p_{3/2}$ state whereas peaks centred around 719, 723.8, 725.8 eV can be attributed to the Fe^o, Fe^{2+}, Fe^{3+} $2p_{1/2}$ states.[1-8] Besides, a Fe^{2+} satellite peak at 715.2 eV ($2p_{3/2}$) has been observed.[6] Similarly, the peaks centred around 853.1, 855.1, 857.2 eV can be attributed to the Ni^o, Ni^{2+}, Ni^{3+} $2p_{3/2}$ state whereas peaks centred around 870.5, 872.5, 874.8 eV can be attributed to the Ni^o, Ni^{2+}, Ni^{3+} $2p_{1/2}$ states.[6-13] In addition, Ni^{2+} satellite peak at 861.7 eV ($2p_{3/2}$) has been also observed.[6]

Table S1. Elemental composition of FNMR (M=3, 10, 25, 40) evaluated from XPS spectra.

Electrocatalyst	**Carbon (at. %)**	**Nitrogen (at. %)**	**Iron (at. %)**	**Nickel (at. %)**
FN3R	90.9	8.1	0.8	0.2
FN10R	89.6	8.4	0.9	1.1
FN25R	84.6	10.8	3.9	0.7
FN40R	90.3	8	0.8	0.9

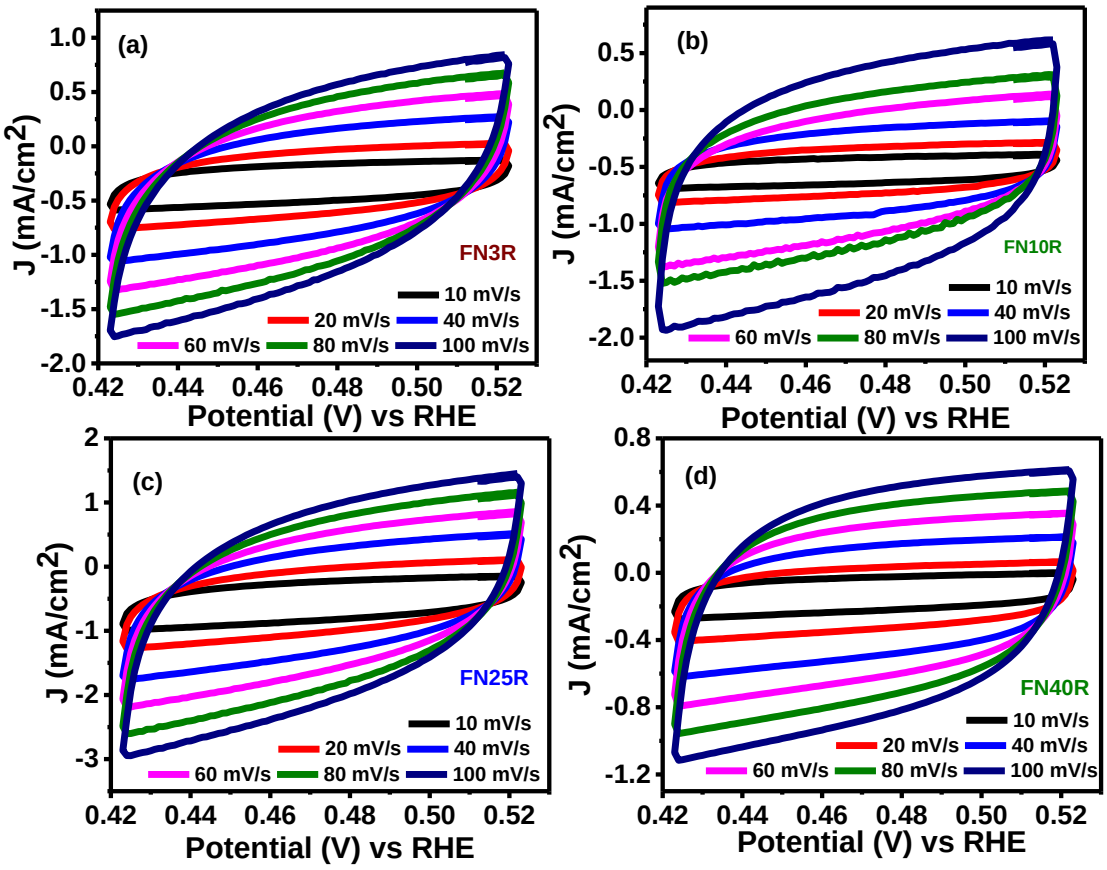

Figure S5. Cyclic voltammograms recorded in non-Faradic region for double layer capacitance calculation in 1 M NaOH nitrogen-purged aqueous solution at different scan rate (10-100 mV/s) for (a) FN3R, (b) FN10R, (c) FN25R and (d) FN40R, respectively.

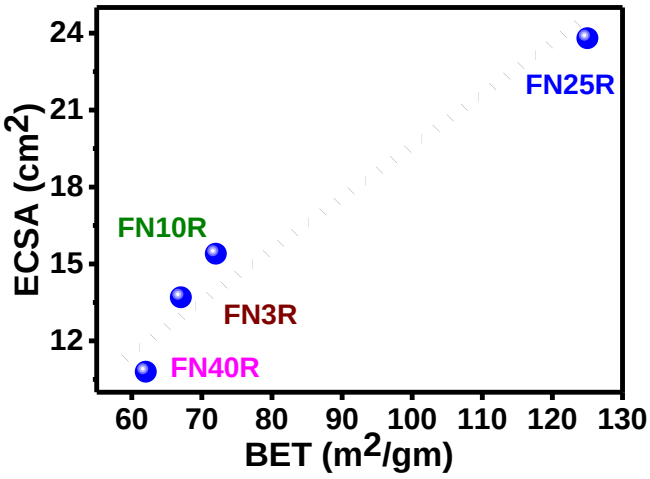

Figure S6. Correlation between BET specific surface area and ECSA. The BET specific surface area is in consistent with the ECSA of FNMR. The line is the guide for eye.

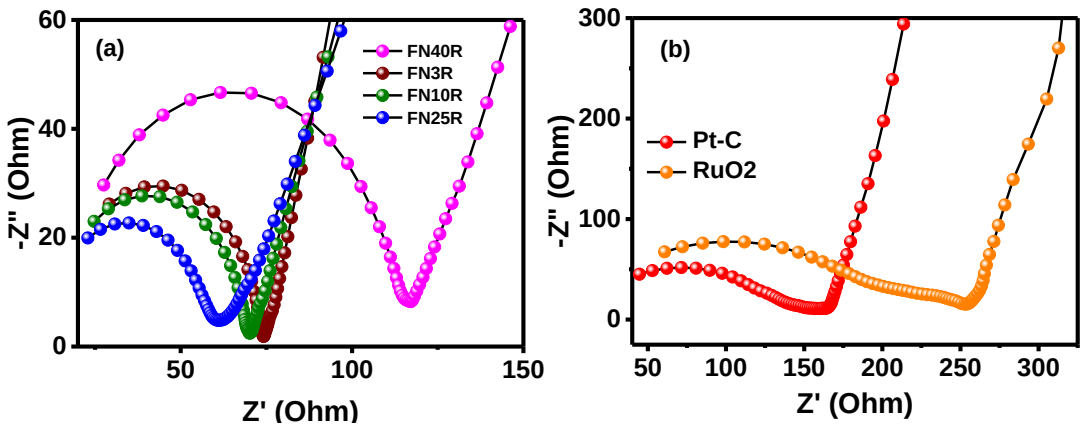

Figure S7. Nyquist plots on (a) FNMR (M=3, 10, 25, 40) and on (b) Pt-C and RuO_2 in 1 M NaOH aquous solution at 1.5 V vs RHE.

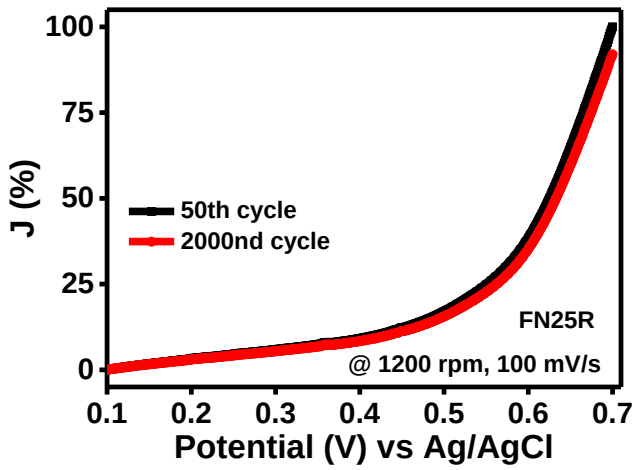

Figure S8. OER polarization curves (50th and 2000nd cycles) recorded on FN25R during accelerated stability test in alkaline (1 M NaOH) medium at rotation speed of 1200 rpm and 100 mV/s scan speed.

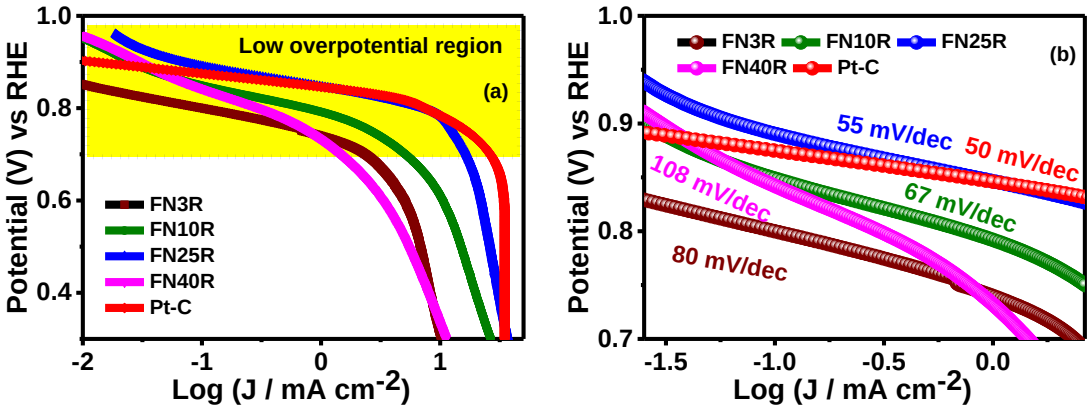

Figure S9. (a) Tafel slope evaluation on FNMR (M= 3, 10, 25, 40) deduced from LSV-ORR polarization curves (from figure 5a) in low over potential region (figure b, magnified portion as marked in figure a).

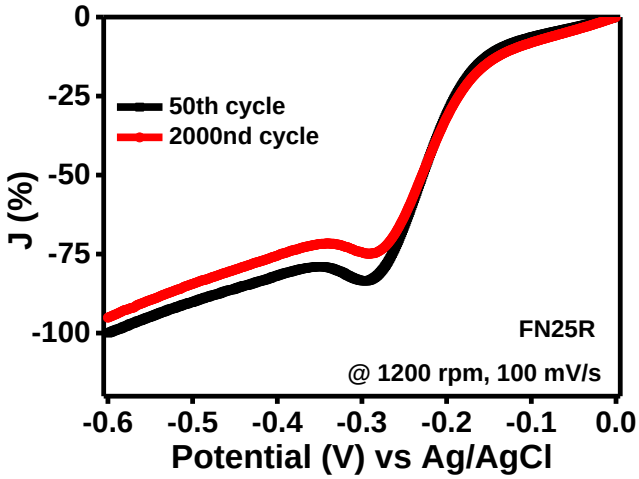

Figure S10. ORR polarization curves (50th and 2000nd cycles) recorded on FN25R during accelerated stability test in alkaline (0.1 M NaOH) medium at rotation speed of 1200 rpm and 100 mV/s scan speed.

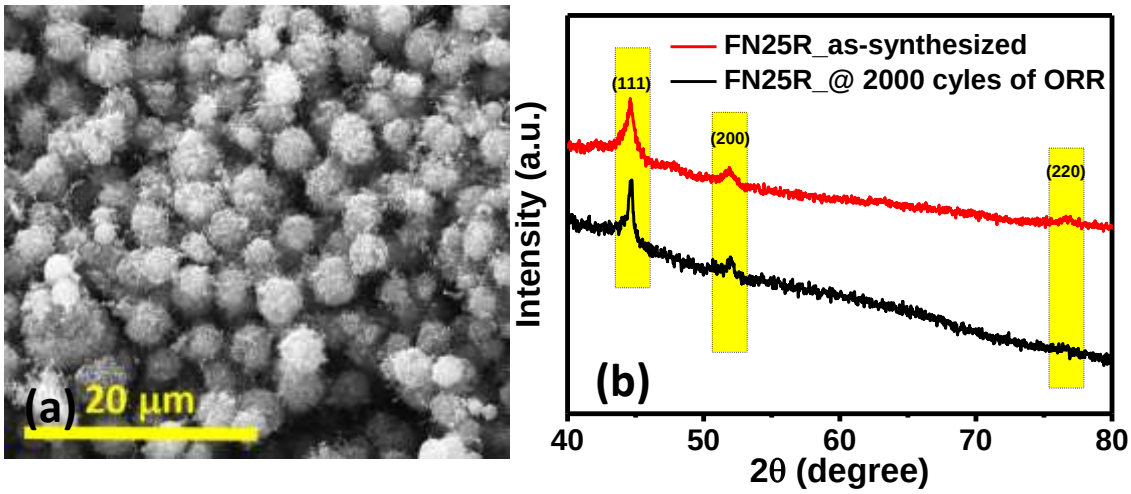

Figure S11. (a) SEM image and (b) XRD pattern recorded on FN25R after ORR-AST study suggest the retaining of structure. The XRD patterns suggests that FeNi nanoparticles present in FN25R preserved the face-centred cubic phase as evident by characteristic reflections arising from (111), (200) and (220) planes of FeNi nanoparticles.

Table S2. OER activity summary for various carbon-based electrocatalysts in alkaline medium.

Electrocatalyst	Electrocatalyst loading	E_{on-set} (mV) Vs Ag/AgCl	$E_{J=10}$ (mV) Vs Ag/AgCl	Reference
$CoFe_2O_4$/rGO	1.006 mg/cm^2	540	700	*Journal of Power Sources 250 (2014) 196-203*
$FeCo_2O_4$-HrGOS	1.006 mg/cm^2	570	750	*Carbon 92 (2015) 74 –83*
$CoFe_2O_4$/CNTs	1.006 mg/cm^2	600	700	*Electrochimica Acta 177 (2015) 65–72*
MWCNT@S–N–C	0.200 mg/cm^2	600	700	*New J. Chem., 2015, 39, 6289--6296*
S,N,Fe-porous carbon	0.100 mg/cm^2	----	650	*Green Chem., 2016, **18**, 4004-4011*
N-doped Fe-Fe_3C@ graphitic layer	0.710 mg/cm^2	600	778	*Green Chemistry 18 (2016), 427-432*
Nitrogen-doped Fe/Fe_3C@graphitic layer/carbon nanotube	0.103 mg/cm^2	500	850	*Chem. Commun., 2015, **51,** 2710-2713*
$NiCo_2S_4$@N/SrGO	0.283 mg/cm^2	600	720	*ACS Appl. Mater. Interfaces*, 2013, 5 (11), pp 5002–5008
Fe_3C-NCNTs co-embedded boron doped carbon	0.75 mg/cm^2	422	562	*J. Mater. Chem. A, 2017, **5**, 16843-16853*
Fe_3C-FeNx enriched carbon sphere	1 mg/cm^2	380	550	*J. Mater. Chem. A, 2018, 6, 8537*
FN10R	0.4 mg/cm^2	465	545	*Present study*
FN25R	**0.4 mg/cm^2**	**375**	**495**	***Present study***

Table S3. ORR activity summary for various carbon-based electrocatalysts in alkaline medium.

Electrocatalyst	Electrocatalyst loading	Eon-set (mV) Vs (Ag/AgCl)	E1/2 (Vs Ag/AgCl)	Reference
MWCNT@S–N–C	0.1 mg/cm^2	-200	~-350	*New J. Chem., 2015, 39, 6289--6296*
$CoFe_2O_4$/CNTs	1.006 mg/cm^2	-124	~ -300	*Electrochimica Acta 177 (2015) 65–72*
$CoFe_2O_4$/rGO	1.006 mg/cm^2	-136	~ -260	*Journal of Power Sources 250 (2014) 196e203*
Co–N–GN	0.1 mg/cm^2	-98	-162	*J. Mater. Chem. A, 2013, **1**, 3593-3599*
N,P,S-rGO/*E. coli*	0.510 mg/cm^2	-90	~ -220	*J. Mater. Chem. A 2015,3, 12873-12879*
$FeCo_2O_4$-HrGOS	1.006 mg/cm^2	-90	~ -200	*Carbon 92 (2015 74-83*
N-graphene/CNT hybrids	0.430 mg/cm^2	-80	~ -200	*Angew. Chem. Int. Ed. 2014, 53, 6496 - 6500*
N-CNTs	0.306 mg/cm^2	-60	-220	*Carbon 50 (2012) 2620-2627*
N,S-Graphene	0.43 mg/cm^2	-60	-300	*Angew. Chem., Int. Ed., 2012, 51, 11496*
Fe_3C-NCNTs co-embedded boron doped carbon	0.75 mg/cm^2	-30	-225	*J. Mater. Chem. A, 2017, **5**, 16843-16853*
FN10R	0.4 mg/cm^2	-65	-265	*Present study*
FN25R	**0.4 mg/cm^2**	**-27**	**-154**	***Present study***

Table S4. Overall oxygen electroactivity (ΔE) summary for various carbon-based electrocatalysts in alkaline medium.

Catalyst	Overall oxygen electrochemistry ΔE ($E_{j=10(OER)} - E_{1/2(ORR)}$)(V)	Reference
S-N-C@MWNCNTs	~1.25	*New J. Chem. 2015, 39, 6289.*
NCNF-1000	~1.02	*Adv. Mater. 2016, 28, 3000−3006.*
Fe/Fe3C@NGL-NCNT	~1	*Chem. Commun. 2015, 51, 2710.*
N-Graphene/CNTs	~1.00	*Small, 2014, 10, 2251.*
B-MWNCNTs	~1.00	*Electrochimica Acta 2014,143, 291.*
$CoFe_2O_4$/rGO	~0.98	*J. Power Sources 2014, 250, 196.*
$CoFe_2O_4$/N-P-biocarbon	~0.98	*J. Mater. Chem. A 2014,2,18012.*
N,P-Carbon paper	~ 0.96	*Angew. Chem. Int. Ed. 2015, 54, 4646.*
P-doped g-C3N4 /CF	~0.96	*Angew. Chem. Int. Ed. 2015, 54, 4646−4650.*
Fe/Fe3C@ N-graphitic layer	~ 0.97	*Green Chemistry 2015, DOI: 10.1039/c5gc01405k*
Pt@C	~0.94	*Angew. Chem. Int. Ed. 2014, 53, 8508.*
Mn_xO_y/N-Carbon	~0.93	*Angew. Chem. Int. Ed. 2014, 53, 8508.*
Ir@C	~0.92	*J. Am. Chem. Soc. 2010,132, 3612.*
$NiCo_2O_4$/Graphene	~0.915	*J. Mater. Chem. A 2013,1,4754.*
N, S, O carbon nanosheet	~0.88	*Nano Energy 19 (2016) 373–381*
Fe@N-C	~0.88	*Nano Energy 2015, 13, 387−396.*
NiO/CoN PINWs	~0.8	*ACS Nano*, 2017, 11 (2), pp 2275–2283
Fe/N/C@BMZIF	~0.79	*ACS Appl. Mater. Interfaces*, 2017, 9 (6), 5213–5221
Fe_3C-NCNTs co-embedded boron doped carbon	~0.788	*J. Mater. Chem. A, 2017, 5, 16843-16853*
Ni_3Fe/N-C sheets	0.84	*Adv. Energy Mater.* 2017, *7*, 1601172
Fe_3C-FeNx enriched carbon sphere	~0.758	*J. Mater. Chem. A, 2018, 6, 8537*
FN25R	**~0.71**	***Present study***

References

[1] R. Nandan, A. Gautam and K. K. Nanda, *J. Mater. Chem. A*, 2017, **5**, 20252–20262;

[2] R. Nandan, A. Gautam, S. Tripathi and K. K. Nanda, *J. Mater. Chem. A*, 2018, 8537–8548.

[3] R. Nandan and K. K. Nanda, *J. Mater. Chem. A*, 2017, **5**, 16843–16853

[4] M. Wang, T. Qian, J. Zhou and C. Yan, *ACS Appl. Mater. Interfaces*, 2017, **9**, 5213–5221.

[5] J.-S. Li, S.-L. Li, Y.-J. Tang, M. Han, Z.-H. Dai, J.-C. Bao and Y.-Q. Lan, *Chem. Commun.*, 2015, **51**, 2710–2713.

[6] X. Wang, X. Liu, C.-J. Tong, X. Yuan, W. Dong, T. Lin, L.-M. Liu and F. Huang, *J. Mater. Chem. A*, 2016, **4**, 7762–7771.

[7] L. Du, L. Luo, Z. Feng, M. Engelhard, X. Xie, B. Han, J. Sun, J. Zhang, G. Yin, C. Wang, Y. Wang and Y. Shao, *Nano Energy*, 2017, **39**, 245–252

[8] F. W. Zhengping Zhang, Yeshen Qin, Meiling Dou, Jing Ji and State, *Nano Energy*, 2016, **30**, 426–433.

[9] C. Xuan, J. Wang, W. Xia, J. Zhu, Z. Peng, K. Xia, W. Xiao, H. L. Xin and D. Wang, *J. Mater. Chem. A*, 2018, 7062–7069.

[10] B. K. Kang, M. H. Woo, J. Lee, Y. H. Song, Z. Wang, Y. Guo, Y. Yamauchi, J. H. Kim, B. Lim and D. H. Yoon, *J. Mater. Chem. A Mater. energy Sustain.*, 2017, **5**, 4320–4324.

[11] H. Qiao, J. Yong, X. Dai, X. Zhang, Y. Ma, M. Liu, X. Luan, J. Cai, Y. Yang, H. Zhao and X. Huang, *J. Mater. Chem. A*, 2017, **5**, 21320–21327.

[12] X. Long, Z. Ma, H. Yu, X. Gao, X. Pan, X. Chen, S. Yang and Z. Yi, *J. Mater. Chem. A*, 2016, **4**, 14939–14943.

[13] U. Y. Qazi, C. Z. Yuan, N. Ullah, Y. F. Jiang, M. Imran, A. Zeb, S. J. Zhao, R. Javaid and A. W. Xu, *ACS Appl. Mater. Interfaces*, 2017, **9**, 28627–28634.